

Effective engine technologies for optimum efficiency and emission control of the heavy-duty diesel engine

Zhibo Ban¹, Wei Guan^{1,2}, Xinyan Wang², Hua Zhao², Tiejian Lin¹, Zunqing Zheng^{2,3}

¹Guangxi Yuchai Machinery Company, Yulin, China

²Brunel University London, London, United Kingdom

³Tianjin University, Tianjin, China

Abstract

The new emissions legislation for the heavy-duty (HD) diesel engine will require cutting NO_x emissions by 90% to 0.02 g/bhp.hr, which is heavily relied upon the effective operation of the SCR in the aftertreatment systems (ATS). However, the low exhaust gas temperature (EGT) at low-load operation usually impedes the efficient exhaust emissions reduction by these aftertreatment systems, which require a minimum EGT of approximately 200°C to initiate the emission control operations.

In this research, studies have been carried out on the effectiveness and trade-off of the advanced combustion control strategies, such as Miller cycle, internal (iEGR) and external exhaust gas recirculation (eEGR), on the engine efficiency, emissions, and EGT management at low-load operation. Experiments were performed on a single-cylinder HD diesel engine equipped with a high-pressure loop cooled eEGR and a variable valve actuation (VVA) system. The VVA system enables the Miller cycle operation with variable later intake valve closing (LIVC) and produces iEGR via a second intake valve opening (2IVO) event during the exhaust stroke.

The results show that common techniques such as the retarded injection timing, intake throttling, iEGR combined with high exhaust back pressure could increase the EGT but at the expense of high fuel consumption and deteriorating the combustion process. In comparison, the Miller cycle operation could increase EGT to more than 200°C with insignificant impact on the net indicated efficiency (NIE). However, the resulting lower effective compression ratio (ECR) decreased the combustion gas temperature, leading to higher hydrocarbon (HC) and carbon monoxide (CO) emissions. The combined Miller cycle with iEGR helped to reduce CO and HC emissions but this strategy demonstrated a limited NO_x emissions reduction, particularly when the injection timing was optimised to achieve the maximum NIE. The introduction of 26%eEGR on the Miller cycle operating with iEGR decreased NO_x emissions by 50%, on average, but presented insignificant impact on the NIE and EGT. When introducing a higher eEGR of 44%, the NO_x emissions were substantially decreased while increasing the EGT to more than 200°C with a higher NIE. However, these were attained with an increase in soot emissions. The additional results demonstrated that the optimised Miller cycle operating with iEGR and eEGR of 44% achieved the highest EGT of 225°C and the lowest NO_x emissions of 0.5 g/kWh but with a soot emissions of 0.026 g/kWh. Alternatively, Miller cycle operating with eEGR of 44% and with no iEGR achieved the highest NIE of 43.7% and the lowest total fluid (fuel and urea) consumption of 0.83 kg/h as well as increasing the EGT to 216°C. Meanwhile, the soot and NO_x emissions were

decreased to below 0.01 g/kWh and 0.79 g/kWh, respectively. Thus, the Miller cycle operating with iEGR and eEGR have been identified as the most effective means of achieving simultaneous higher engine efficiency, lower emissions, and desired EGT, substantially improving the effectiveness of ATS at the low-load operation.

Keywords

Heavy-duty diesel engine, Miller cycle, EGR, aftertreatment, total fluid consumption, exhaust gas temperature

1. Introduction

Due to the superior traction properties with high torque output and low fuel consumption, diesel engines have been the dominant powerplant for heavy-duty (HD) vehicles and many other applications. The existence of locally fuel-rich and high combustion temperature zones resulted from the non-premixed diffusion-controlled combustion in the conventional diesel combustion, however, lead to the emission of particulate matter (PM) and nitrogen oxides (NO_x) [1,2]. As more vehicles are produced and used with the increased economic development and prosperity in both developed and developing countries, it is necessary to reduce CO₂ emission and pollutant emissions as reflected by the introduction of more stringent emission regulations. In particular, the US EPA has recently finalized their Phase 2 HD greenhouse gas (GHG) regulation, which requires about 5% reductions in carbon dioxide (CO₂) compared to Phase 1 [3]. Additionally, the California Air Resource Board is continuing to move forward with cutting HD NO_x emissions up to 90% to 0.02 g/bhp-hr from new trucks by about 2024, which is significantly lower than the current limit of 0.2 g/bhp-hr [4,5].

These legislative trends described above put forward higher requirements for diesel engine development and require further research work in engine and aftertreatment technologies in order to simultaneously decrease NO_x emissions and improve net indicated efficiency (NIE). Moreover, aftertreatment systems such as NO_x selective catalytic reduction (SCR) system, diesel particulate filter (DPF), and diesel oxidation catalyst (DOC) are strongly dependent on the exhaust gas temperature (EGT). A minimum EGT of approximately 200°C is required for catalyst light-off and to initiate the emissions control [6,7]. This is extremely challenging at low-load conditions as the EGT is too low to provide sufficient emissions reduction [8]. Advanced combustion technologies such as the multiple fuel injection strategy, higher fuel injection pressure, and higher boost pressure have been employed to improve upon NIE, however, these technologies are typically accompanied with a lower EGT [9].

Miller cycle has recently been adopted for in-cylinder NO_x reduction and exhaust gas temperature management of diesel engines, though the Miller cycle was originally patented for the boosted spark ignition gasoline engine by Ralph Miller in 1957 [10]. Compared to the other more conventional techniques such as the retarded injection timing [11], post injection [12], and intake throttling [13], Miller cycle is an effective technology for NO_x emissions and EGT control, particularly at the low engine load operation in the HD diesel engine [14–17]. This is due to the fact that Miller cycle implemented via either early or late intake valve dosing (IVC) timings reduces the effective compression ratio and intake charge, resulting in a reduction in peak in-cylinder combustion temperature and air-fuel ratio. Previous studies have demonstrated the capability of Miller cycle to reduce the engine-out NO_x emission, the level of NO_x reduction achieved by Miller cycle alone is limited and less than EGR, particularly at low engine loads [18]. In addition, the resulting lower in-cylinder pressure and temperature at the start of combustion lead to poor combustion stability and higher CO and unburned HC emissions. Alternatively, the

iEGR realised via a 2nd IVO during the exhaust stroke and/or exhaust valve re-opening (2EVO) during the intake stroke can retain hot residuals from the previous cycle. The combined use of iEGR and Miller cycle operation enabled exhaust thermal management with low levels of unburned HC and CO emissions [19–21], but with insufficient NO_x emissions reduction, as reported in our previous works [22].

Cooled external EGR is a proven technology for the reduction in NO_x formation in the cylinder, because of their thermal, chemical, and dilution effects [23,24]. Previous studies have investigated the combined use of Miller cycle and EGR and have demonstrated that this strategy is effective in curbing engine-out NO_x emissions [25,26]. Kim et al. [18] showed that the combined use of Miller cycle with EGR could reduce the NO_x emissions from 10 g/kWh to approximately 1 g/kWh at low load operation. Similar results were reported by Verschaeren et al. [27] on the use of Miller cycle and EGR in a HD diesel engine.

To address the challenges encountered by current HD diesel engines at low-load operation, research and development work is required to further optimise the combustion process to achieve simultaneous reduction in fuel and urea consumption. This paper will present the results obtained with different advanced combustion control strategies and analyse their effectiveness to improve upon exhaust gas temperatures and reduce emissions as well as to increase NIE and reduce total fluid consumption at low-load operation. The experimental study was carried out on a single cylinder HD diesel engine at an engine speed of 1150 rpm and engine load of 2.2 bar net indicated mean effective pressure (IMEP). The conventional strategies such as the retarded injection timing and intake throttling for EGT management were investigated and compared to the Miller cycle and iEGR. Moreover, the influence of Miller cycle operating with internal and external EGR on the engine combustion, performance, and emissions was investigated. Finally, an overall engine efficiency and exhaust emissions analysis of various combustion control strategies was analysed and the optimised engine combustion control strategies were identified.

2. Experimental setup

2.1 Engine specifications and experimental facilities

Figure 2 shows the schematic of the experimental setup in this work, which comprises of a single cylinder engine, the engine test bench, a boosting system, as well as measurement devices and a data acquisition system. In order to absorb the work inputted from the engine, a Froude-Hofmann AG150 Eddy current dynamometer with a rated power of 150 kW and maximum torque of 500 Nm was deployed.

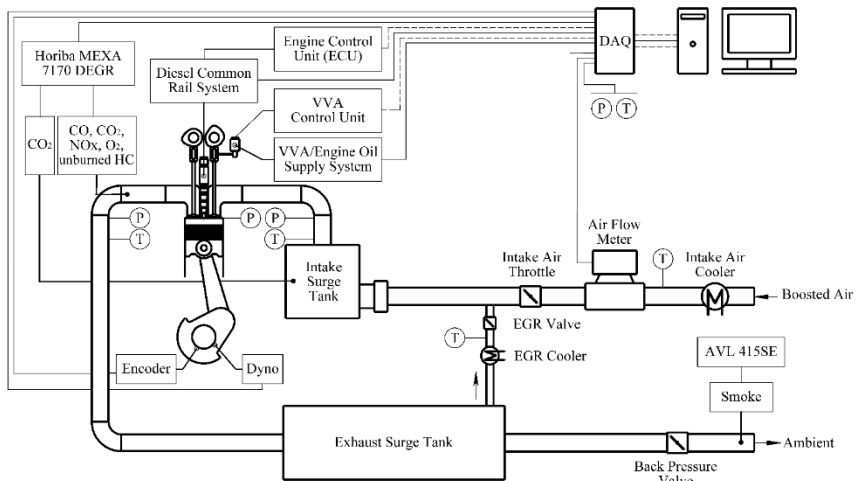


Figure 1. Layout of the engine experimental setup.

Table 1. Specifications of the test engine.

Displaced Volume	2026 cm ³
Stroke	155 mm
Bore	129 mm
Connecting Rod Length	256 mm
Geometric Compression Ratio	16.8
Number of Valves	4
Piston Type	Stepped-lip bowl
Diesel Injection System	Bosch common rail
Nozzle design	8 holes, 0.176 mm hole diameter, included spray angle of 150°
Maximum fuel injection pressure	2200 bar
Maximum in-cylinder pressure	180 bar

The testing engine is typically developed for a modern truck. The key specifications of the engine are listed in Table 1. Amid the composition of the engine, the design of the cylinder head with 4-valve and a stepped-lip piston bowl were based on the Yuchai YC6K six-cylinder engine, while the bottom end/short block was AVL-designed with two counter-rotating balance shafts.

The compressed air was supplied by an AVL 515 sliding vanes supercharger with closed loop control. Two surge tanks were installed to damp out the strong pressure fluctuations in intake and exhaust manifolds, respectively. The intake manifold pressure was finely controlled by a throttle valve located upstream of the intake surge tank. The intake mass flow rate was measured by a thermal mass flow meter. An electronically controlled butterfly valve located downstream of the exhaust surge tank was used to independently control the exhaust back pressure. High-pressure loop cooled external EGR was introduced to the engine intake manifold located between the intake surge tank and throttle by using a pulse width modulation-controlled EGR valve and the pressure differential between the intake and exhaust

manifolds. Water cooled heat exchangers were used to control the temperatures of the boosted intake air and external EGR as well as engine coolant and lubrication oil. The coolant and oil temperatures were kept within 356 ± 2 K. The oil pressure was maintained within 4.0 ± 0.1 bar throughout the experiments.

During the experiments, the diesel fuel was injected into the engine by a high-pressure solenoid injector through a high pressure pump and a common rail with a maximum fuel pressure of 2200 bar. A dedicated electronic control unit (ECU) was used to control fuel injection parameters such as injection pressure, start of injection (SOI), and the number of injections per cycle. The fuel consumption was determined by measuring the total fuel supplied to and from the high pressure pump and diesel injector via two Coriolis flow meters. The specifications of the measurement equipment can be found in Appendix A.

2.2 Variable valve actuation system

The engine was equipped with a lost-motion VVA system, which incorporated a hydraulic collapsing tappet on the intake valve side of the rocker arm. This system allowed for the Miller cycle operation via LIVC. The intake valve opening (IVO) and IVC timings of the baseline case were set at 367 and -174 crank angle degrees (CAD) after top dead centre (ATDC), respectively. All valve events were considered at 1 mm valve lift and the maximum intake valve lift event was set at 14 mm.

In addition, this system enables a 2IVO event during the exhaust stroke for the purpose of trapping iEGR in order to increase the residual gas fraction. The earliest opening timing and the latest closing timing of the 2IVO strategy were set at 130 CAD ATDC and 230 CAD ATDC, respectively. The maximum valve lift of this configuration was 2 mm. Figure 2 shows the intake and exhaust valve profiles for the baseline engine operation as well as the LIVC and 2IVO strategies. The effective compression ratio, ECR, was calculated as

$$ECR = \frac{V_{vc,eff}}{V_{tdc}} \quad (1)$$

where V_{tdc} is the cylinder volume at top dead centre (TDC) position, and $V_{vc,eff}$ is the effective cylinder volume where the in-cylinder compressed air pressure is extrapolated to be identical to the intake manifold pressure [28].

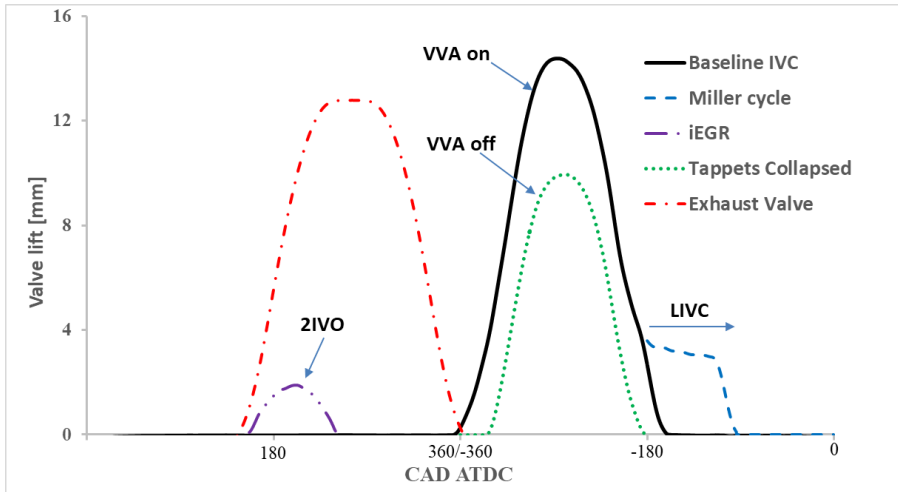


Figure 2. Fixed exhaust and variable intake valve lift profiles.

2.3 Exhaust emissions measurement

A Horiba MEXA-7170 DEGR emission analyser was used to measure the exhaust gases (NO_x, HC, CO, and CO₂). In this analyser system, gases including CO and CO₂ were measured through a non-dispersive infrared absorption (NDIR) analyser, HC was measured by a flame ionization detector (FID), and NO_x was measured by a chemiluminescence detector (CLD). To allow for high pressure sampling and avoid condensation, a high pressure sampling module and a heated line were used between the exhaust sampling point and the emission analyser. The smoke number was measured downstream of the exhaust back pressure valve using an AVL 415SE Smoke Meter. The measurement was taken in filter smoke number (FSN) basis and thereafter was converted to mg/m³ [29]. All the exhaust gas components were converted to net indicated specific gas emissions (in g/kWh) according to [30]. In this study, the eEGR rate was defined as the ratio of the measured CO₂ concentration in the intake surge tank ($(CO_2\%)_{intake}$) to the CO₂ concentration in the exhaust manifold ($(CO_2\%)_{exhaust}$) as

$$eEGR\ rate = \frac{(CO_2\%)_{intake}}{(CO_2\%)_{exhaust}} * 100\% \quad (2)$$

2.4 Data acquisition and analysis

The instantaneous in-cylinder pressure was measured by a Kistler 6125C piezo-electric pressure transducer with a sampling revolution of 0.25 CAD. The captured data from the high speed and low speed National Instruments data acquisition (DAQ) cards as well as the resulting engine parameters were display in real-time by an in-house developed transient combustion analysis software.

The crank angle based in-cylinder pressure traces were recorded through an AVL FI Piezo charge amplifier and was averaged over 200 consecutive engine cycles and used to calculate the IMEP and apparent heat release rate (HRR). According to [1], the apparent HRR was calculated as

$$HRR = \frac{\gamma}{(\gamma - 1)} p \frac{dV}{d\theta} + \frac{1}{(\gamma - 1)} V \frac{dp}{d\theta} \quad (3)$$

where γ is defined as the ratio of specific heats and assumed constant at 1.33 throughout the engine cycle [31]; V and p are the in-cylinder volume and pressure, respectively; θ is the crank angle degree.

In this study, the CA10, CA50 (combustion phasing) and CA90 were defined as the crank angle when the fuel mass fraction burned (MFB) reached 10%, 50%, and 90%, respectively. Combustion duration was represented by the period of time between the crank angles of CA10 and CA90. Ignition delay was defined as the period of time between the SOI and the start of combustion (SOC), denoted as 0.3% MFB point of the average cycle. The in-cylinder combustion stability was monitored by the coefficient of variation of the IMEP (COV_{IMEP}) over the sampled cycles.

3. Methodology

3.1 Estimation of the total fluid consumption

An increase in engine-out NO_x emissions can lead to a higher consumption of aqueous urea solution in the aftertreatment system of an SCR equipped HD diesel engine. This can adversely affect the total engine fluid consumption and thus the engine operational cost. Therefore, the total fluid consumption is estimated in this study in order to take into account both the measured diesel flow rate (\dot{m}_{diesel}) and the estimated urea consumption in the SCR system (\dot{m}_{urea}). As the relative prices between diesel fuel and urea are different in different countries and regions, the price and property of urea is simulated to be the same as diesel fuel in this study [32]. According to Charlton et al. [32] and Johnson [33], the required aqueous urea

solution to meet the Euro VI NO_x limit of 0.4 g/kWh can be estimated as 1% of the diesel equivalent fuel flow per g/kWh of NO_x reduction, i.e.

$$\dot{m}_{urea} = 0.01 * (NO_{x_{Engine-out}} - NO_{x_{EuroVI}}) * \dot{m}_{diesel} \quad (4)$$

The total fluid consumption is then calculated by adding the measured diesel flow rate to the estimated urea flow rate as

$$\dot{m}_{total} = \dot{m}_{urea} + \dot{m}_{diesel} \quad (5)$$

3.2 Test conditions

In this study, the experimental work was carried out at the engine speed of 1150 rpm and light engine load of 2.2 bar IMEP, which represents a typical engine operating condition of a HD drive cycle characterised with low exhaust gas temperature below 200°C. Table 2 summarises the engine test conditions for the different engine combustion control strategies investigated.

The start of injection (SOI) of the baseline engine operation was swept between -11.5 and 2.5 CAD ATDC to achieve the maximum fuel efficiency and EGT of 200°C. In the intake throttling mode, the intake pressure was gradually decreased while maintaining the exhaust pressure constant. During the engine operation with iEGR via 2IVO, the exhaust back pressure was varied to increase the residual gas fraction while the intake pressure was held constant at 1.15 bar. Miller cycle operation was achieved via late intake valve closure (LIVC) and the IVC timing was swept to estimate the effectiveness of Miller cycle on the EGT management. For the Miller cycle operating with iEGR and eEGR, the SOI was optimised to achieve the maximum fuel efficiency. When the EGR rate of 44% was introduced, the Miller cycle was operated under naturally aspirated conditions with an intake pressure of 0.98 bar. This setting was necessary in order to isolate the influence on the turbocharger operation and to analyse the feasibility of these strategies in a production multi-cylinder engine. Stable engine operation was determined by controlling the COV_{IMEP} below 3%.

Table 2 Engine test conditions for various combustion control strategies.

Testing modes	Speed (rpm)	Load (bar IMEP)	Injection pressure (bar)	SOI (CAD ATDC)	Intake pressure (bar)	Exhaust pressure (bar)	IVC (CAD ATDC)	2IVO	eEGR (%)
Baseline	1150	2.2	510	Swept	1.15	1.20	-178	off	0
Intake throttling				-5.8	Swept	1.20	-178	off	0
iEGR				-5.8	1.15	Swept	-178	on	0
Miller cycle				Swept	1.15	1.20	Swept	off	0
Miller cycle + iEGR				Swept	1.15	1.20	-100	on	0
Miller cycle + iEGR + 26%eEGR				Swept	1.15	1.20	-100	on	26
Miller cycle + iEGR + 44%eEGR				Swept	0.98	1.08	-100	on	44
Miller cycle + 44%eEGR				Swept	0.98	1.08	-100	off	44

4. Results and discussions

4.1 Estimation of the effectiveness of various combustion control strategies

In this section, conventional techniques such as the retarded injection timing, intake throttling as well as the VVA based strategies including Miller cycle and iEGR are analysed and compared, in terms of their effectiveness on exhaust gas temperature management and the impacts on the fuel conversion efficiency and exhaust emissions.

Figure 3 shows an overview of the increase in EGT versus the percentage variation in fuel consumption of the different combustion control strategies when compared to the baseline case operating with the maximum fuel efficiency. It demonstrated that by delaying the combustion phasing through retarded injection timing, the EGT was increased at the expense of fuel efficiency penalty, leading to the highest fuel consumption when the EGT was increased to reach 200°C. For the intake throttling and iEGR strategies, the EGT could be increased to more than 200°C, but with lower NIE. This was a result of the increased pumping loop areas attributed to the lower intake manifold pressure in the intake throttling strategy and higher exhaust back pressure in the iEGR strategy, as demonstrated in our previous work [22].

In comparison, Miller cycle via LIVC strategy operating with and without iEGR were more effective in increasing EGT with lower fuel efficiency penalty. However, the application of Miller cycle significantly increased the unburned HC and CO emissions, as shown in Figure 4. This is because of the lower effective compression ratio and a reduction in the combustion temperature. Although the introduction of iEGR to the Miller cycle operation could substantially reduce both CO and unburned HC emissions, the capability of curbing NOx emissions was insufficient. Therefore, a cooled external EGR was introduced in an attempt to achieve lower level of engine-out NOx emission while improving upon the fuel efficiency and EGT management in the next section of study.

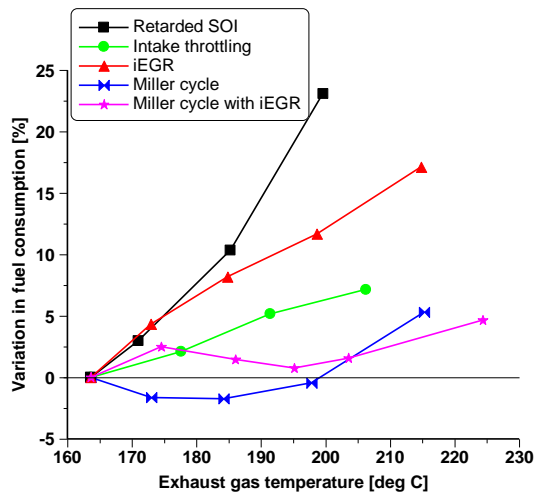


Figure 3. Comparison of the effectiveness of various strategies for EGT management.

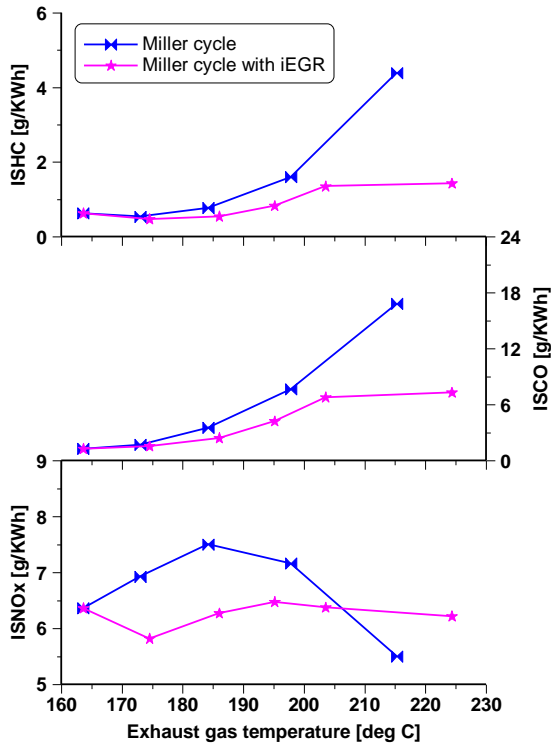


Figure 4. Effect of Miller cycle operating with and without iEGR on emissions.

4.2 Analysis of the in-cylinder pressure and heat release rate

According to the discussion and analysis in the above section, Miller cycle with iEGR strategy has been demonstrated as an enabling technology for efficient increase in the EGT while maintaining reasonable fuel consumption penalty when compared to others. To further reduce the levels of engine-out NOx emissions, the eEGR was introduced to the Miller cycle operating with iEGR.

Figure 5 shows the in-cylinder pressure and HRR profiles for the baseline and the cases of Miller cycle operating with iEGR and eEGR. The comparison was performed with the maximum NIE achieved via optimising the injection timing (SOI). The optimised SOI of the Miller cycle combined with iEGR strategy was later than that of the baseline case. This strategy led to the most retarded heat release but the highest peak HRR attributed to the higher degree of pre-mixed combustion. The addition of eEGR advanced the optimised SOI and thus the start of combustion, especially when the eEGR of 44% was employed. It can be also seen that the iEGR advanced the SOC of the Miller cycle with eEGR of 44% at a constant SOI. This was due to the hot residual gas introduced via iEGR, which increased the gas temperature during the compression stroke. In comparison to the baseline operation, Miller cycle operating with iEGR and eEGR significantly decreased the in-cylinder pressure, particularly in the cases with the higher eEGR of 44%. The peak HRR was apparently higher than the baseline engine operation due to the increased percentage of pre-mixed combustion.

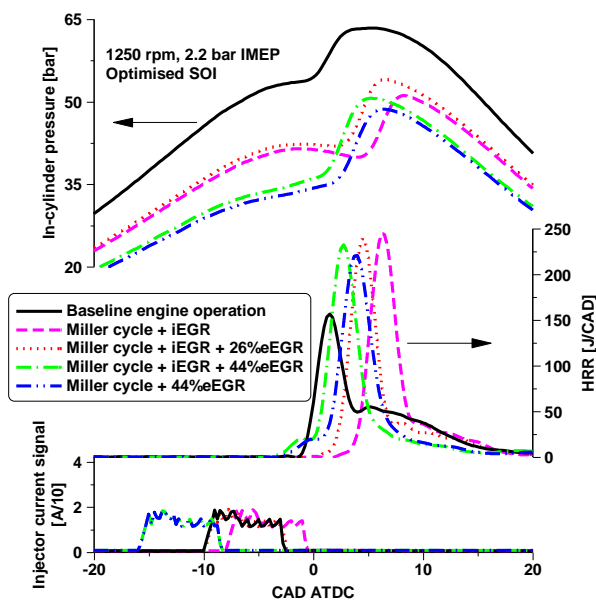


Figure 5. In-cylinder pressure, HRR, and diesel injection signal for the optimum baseline and Miller cycle operating with iEGR and eEGR cases.

4.3 Combustion characteristics

Figure 6 depicts the diesel injection timing and the resulting combustion characteristics as a function of the variation in EGT for the different combustion control strategies.

Compared to the optimum baseline case, the retarded SOI strategy achieved the minimum EGT requirement of 200°C at a very late SOI. This led to a substantially later combustion phase and an unstable combustion process represented by an increase in the COV_{IMEP} to more than 3%. The combined use of Miller cycle and iEGR allowed for a relatively earlier SOI to achieve the minimum required EGT, but the combustion phasing and CA₉₀ were delayed when compared to those of the optimum baseline case. The lower ECR resulted from the LIVC and the higher total heat capacity due to the use of iEGR lengthened the ignition delay as the EGT was increased. This increased the degree of pre-mixed combustion and thus led to a faster combustion rate, resulting in a shorter combustion duration.

The introduction of a moderate eEGR of 26% on the Miller cycle operation with iEGR produced insignificant impact on the combustion characteristics. When the eEGR was increased to 44%, the EGT was raised to more than 200°C with the optimised SOI. In addition, the resulting CA₅₀ and CA₉₀ were held similar to those of the optimum baseline operation. These were because the use of a relatively higher eEGR of 44% produced higher impact on the combustion process attributed to the stronger dilution, heat capacity, and chemical effects. Consequently, the ignition delay was increased by 4 CAD, on average, compared to the baseline case with the optimised SOI. It can be also seen that the ignition delay was longer and the combustion duration was shorter when Miller cycle operating with eEGR of 44% and with no iEGR. Overall, all Miller cycle cases were performed with COV_{IMEP} of below 3%.

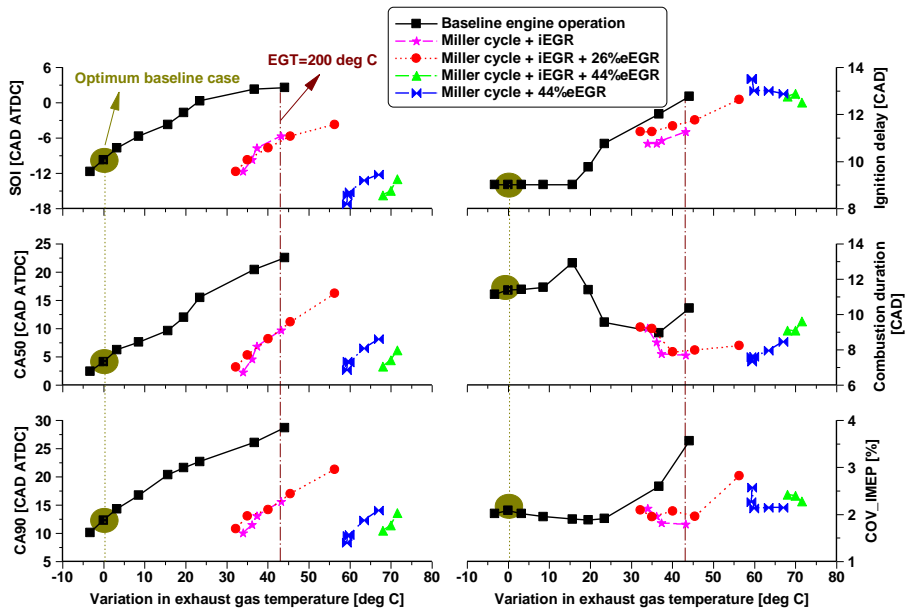


Figure 6. Injection timing and combustion characteristics of the baseline and Miller cycle operating with iEGR and eEGR.

4.4 Engine performance

Figure 7 shows the engine performance parameters for the baseline and Miller cycle operating with iEGR and eEGR. The intake pressure was held constant at 1.20 bar except for those cases performed with a higher eEGR of 44%, where the engine was operated under the naturally aspirated conditions. As a result, the intake air mass flow rate was dropped from 90 kg/h in the baseline operation to approximately 30 kg/h in those cases of Miller cycle operating with high eEGR. The variation in lambda presented a similar trend to the intake air mass flow rate, decreasing from 5.1 to 1.9, on average. The Miller cycle operating with high eEGR produced relatively higher pumping mean effective pressure (PMEP), as a higher pressure differential of 10 kPa between intake and exhaust manifolds was employed compared to the 4 kPa used in the other operating modes.

The retarded SOI strategy apparently decreased the combustion efficiency as the EGT was increased. The combustion efficiency was reduced from 99.6% in the optimum baseline case to 95.8% when the SOI was delayed to achieve the minimum required EGT of 200°C. This resulted in a lower NIE of 35.7% than the 42.1% in the optimum baseline case. The Miller cycle with iEGR strategy maintained the high combustion efficiency and achieved slightly higher NIE when achieving the minimum required EGT. This was attributed to the higher degree of pre-mixed combustion and shorter combustion duration, which improved the combustion process and minimised the heat losses. The introduction of a moderate eEGR of 26% produced insignificant impact on the combustion efficiency and NIE when the EGT was increased to 200°C. When a higher eEGR of 44% was introduced, however, the NIE was improved while achieving a higher EGT of more than 200°C, despite a higher PMEP and a slightly lower combustion efficiency than the optimum baseline case. This was also attributed to a higher degree of pre-mixed combustion and a shorter combustion duration. Figure 7 also shows that the Miller cycle operating with eEGR of 44% and with no iEGR achieved higher NIE than those cases operated with iEGR. This was because the trapped hot residual gas via 2IVO

advanced the SOC and thus shortened the ignition delay, decreasing the degree of pre-mixed combustion and lengthening the combustion duration, as demonstrated in Figure 6.

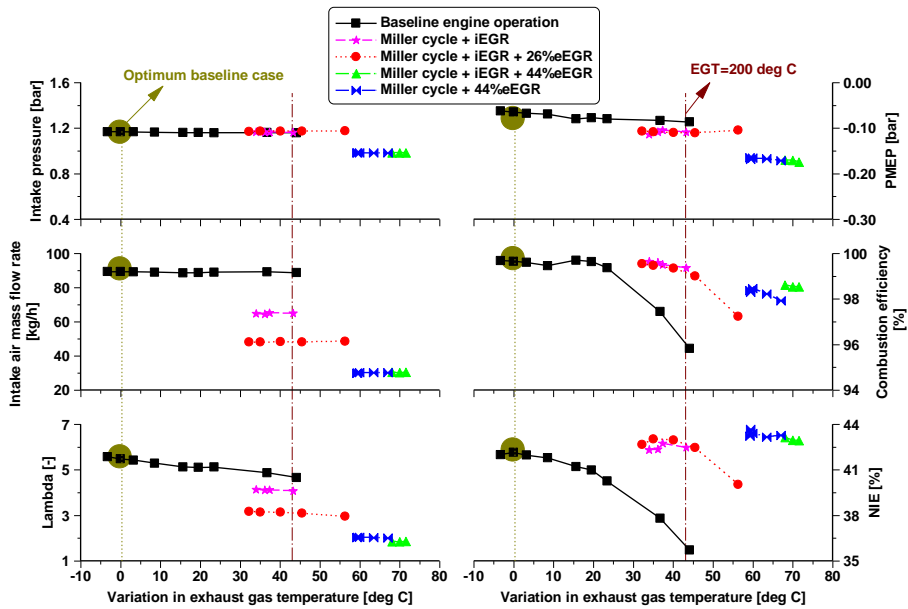


Figure 7. Engine performance parameters of the baseline and Miller cycle operating with iEGR and eEGR.

4.5 Engine-out emissions

Figure 8 depicts the engine-out emissions characteristics as a function of the variation in EGT for the different combustion control strategies. The retarded SOI decreased the NO_x and soot emissions but produced substantially higher unburned HC and CO emissions due to the very late combustion process and much lower combustion temperature. The Miller cycle operating with iEGR achieved lower levels of soot, unburned HC, and CO emissions, but with a limited capability of NO_x emissions reduction. The introduction of 26% eEGR decreased the NO_x emissions by 50% from 6 g/kWh in the Miller cycle operation with iEGR to 3 g/kWh while maintaining the low levels of soot, unburned HC, and CO emissions. These were attained when the EGT was increased to 200°C. Nevertheless, the combination with the use of a higher eEGR of 44% significantly minimised the NO_x emissions to about 0.5 g/kWh, which is very close to the Euro VI NO_x limit of 0.4 g/kWh. However, this was at the expense of an increase in soot emissions. Alternatively, the Miller cycle operating with eEGR of 44% and with no iEGR decreased the soot emissions to below the Euro VI soot limit of 0.01 g/kWh at the expense of a slightly higher unburned HC and CO emissions.

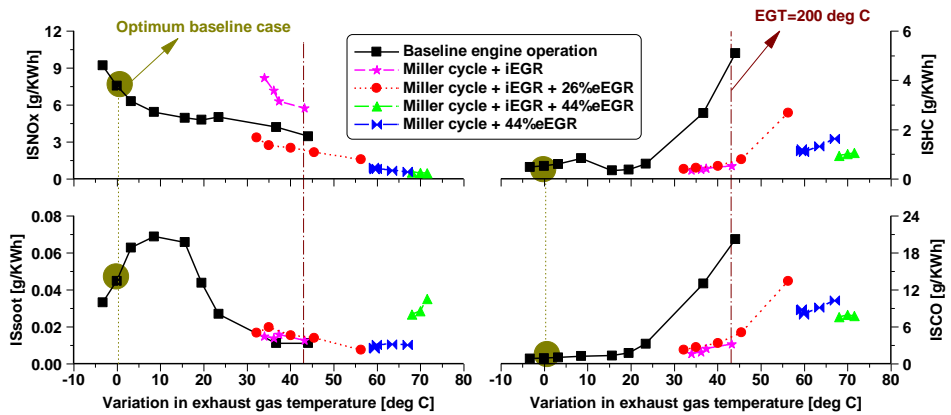


Figure 8. Engine-out exhaust emissions of the baseline and Miller cycle operating with iEGR and eEGR.

4.6 Overall engine efficiency and emissions analysis

In this section, the overall engine efficiency and engine-out emissions of different engine combustion control strategies were analysed by taking into account the consumption of aqueous urea solution in the SCR system. The effectiveness of Miller cycle operating with iEGR and eEGR was estimated and compared to the optimum baseline case.

Figure 9 provides an overall assessment of the potential of the Miller cycle operating with iEGR and eEGR in terms of exhaust emissions, engine performance, and total fluid consumption of a diesel engine operating at low engine load. The results of different combustion control strategies were compared when the SOI was optimised to achieve the maximum NIE. The optimum baseline case was characterised with low EGT of 157°C and NIE of 42.1% as well as high levels of NOx and soot emissions, and thus the highest level in total fluid consumption of 0.87 kg/h. It can be seen that the required urea consumption in the SCR systems closely linked to the level of the engine-out NOx emissions. The reduction in the engine-out NOx emissions by using advanced Miller cycle-based combustion control strategies substantially minimised the requirement on the urea consumption.

Compared to the baseline engine operation, the optimised Miller cycle combined with iEGR slightly increased the NIE and decreased the NOx emissions. Meanwhile, the soot emissions were substantially decreased. However, the EGT was lower than the minimum requirement of 200°C, although an increase in the EGT. The introduction of a moderate eEGR of 26% achieved higher NIE and lower NOx emissions, contributing to a noticeable reduction in the total fluid consumption due to lower fuel and urea consumptions. However, this strategy with optimised SOI produced insignificant impact on the EGT, which was still lower than the minimum requirement. Preferably, the addition of a higher eEGR of 44% achieved higher EGT of 225°C and NIE of 43.1% while significantly reducing the NOx emissions to 0.5 g/kWh. However, these were accompanied with an increase in soot, unburned HC, and CO emissions. Alternatively, the Miller cycle with eEGR of 44% and with no iEGR achieved the highest NIE of 43.7% and the lowest total fluid consumption of 0.83 kg/h while increasing the EGT to 216°C. In the meantime, the soot emissions were decreased to below 0.01g/kWh, but with an increase in unburned HC and CO emissions. The slightly higher CO and unburned HC concentrations could contribute to further increase in the EGT when they are oxidized in the DOC, which operates between 200 and 450°C [8,34].

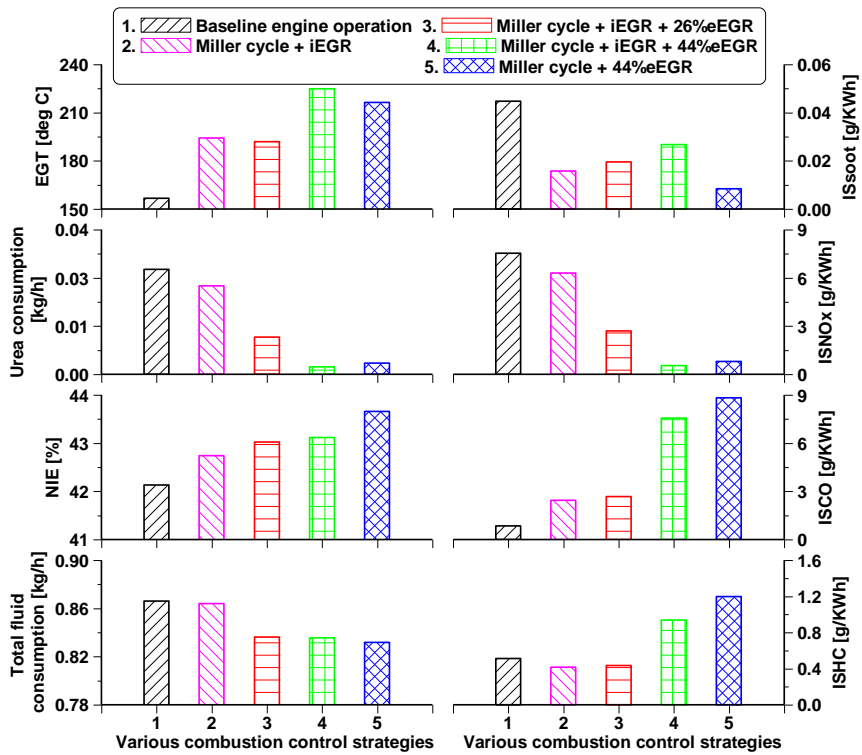


Figure 9. Comparison of the overall engine efficiency and engine-out emissions for various strategies under the condition of achieving maximum NIE.

5. Conclusions

In this study, the effect of Miller cycle operating with iEGR and eEGR on engine combustion process, performance, and exhaust emissions was investigated. Experiments were performed on a HD diesel engine operating at a typical light engine load of 2.2 bar IMEP with low exhaust gas temperature of below 200°C. The aim of the research was to explore alternative combustion control strategies as means to overcome the challenges encountered by current HD diesel engines operating at low engine loads, such as insufficient high EGT for efficient exhaust conversion, low fuel conversion efficiency, and high engine-out emissions. Both Miller cycle and iEGR operations were realised by means of a VVA system. Cooled external EGR and diesel fuel injection strategy were achieved via a high pressure loop EGR and a common rail fuel injection system, respectively. The primary findings can be summarised as follows:

1. Strategies such as retarded SOI, intake throttling, and iEGR were able to increase the EGT to reach the minimum requirement of 200°C, but these strategies decreased the net indicated efficiency (NIE) due to the significantly late combustion process and higher pumping losses accordingly.
2. The Miller cycle operation enabled a higher EGT with little impact on the NIE, but the lower in-cylinder combustion gas temperature resulted in higher levels of unburned HC and CO emissions. The Miller cycle with iEGR was able to improve the combustion process and thus lower HC and CO emissions, but its

capability to minimise NO_x emissions was very limited, especially when the SOI was optimised to achieve the maximum NIE.

3. The introduction of a moderate eEGR of 26% on the Miller cycle with iEGR operation produced insignificant impact on the engine combustion, performance, and exhaust emissions (except for NO_x emissions). When increased the eEGR to 44%, however, the EGT was substantially increased with a higher NIE and significantly lower NO_x emissions. These were attained with an increase in soot, unburned HC, and CO emissions.
4. When comparing at the optimised SOI of various combustion control strategies, the Miller cycle operating with iEGR and eEGR achieved higher NIE and lower engine-out NO_x emissions, which contributed to a reduction in total fluid consumption (fuel and urea). Meanwhile, the EGT was noticeably increased and soot emissions were significantly reduced when compared to the baseline engine operation.
5. Among these strategies investigated, Miller cycle operating with eEGR of 44% and iEGR achieved the highest EGT of 225°C and the lowest NO_x emissions of 0.5 g/kWh. Alternatively, Miller cycle operating with eEGR of 44% and with no iEGR achieved the highest NIE of 43.7% and the lowest total fluid consumption of 0.83 kg/h while increasing the EGT to 216°C and reducing soot emissions to below 0.01 g/kWh. However, these strategies produced higher levels of unburned HC and CO emissions than other engine operation modes.
6. Overall, strategies such as Miller cycle operating with eEGR and iEGR were identified as effective means for EGT management and emissions control as well as efficiency improvement at low-load operation, substantially minimise the total fluid consumption and potentially complying with the future fuel efficiency and ultra-low NO_x emissions regulations.

Contact information

Dr Wei Guan

Email: gwei916@163.com

or

Professor Hua Zhao

Email: hua.zhao@brunel.ac.uk

Centre for Advanced Powertrain and Fuels Research

College of Engineering, Design and Physical Sciences

Brunel University London

Kingston Lane

Uxbridge

Middlesex UB8 3PH

United Kingdom

Acknowledgments

The authors would like to acknowledge the Guangxi Yuchai Machinery Company for supporting and funding this project carried out at Brunel University London.

Declaration of conflicting interests

The author(s) declared no potential conflicts of interest with respect to the research, authorship, and/or publication of this article.

Funding

The author(s) disclosed receipt of the following financial support for the research, authorship, and/or publication of this article: Funding for this project was provided by Guangxi Yuchai Machinery Company.

Definitions/Abbreviations

ATS Aftertreatment System.

ATDC	After Firing Top Dead Center.
CA90	Crank Angle of 90% Cumulative Heat Release.
CA50	Crank Angle of 50% Cumulative Heat Release.
CA10	Crank Angle of 10% Cumulative Heat Release.
CAD	Crank Angle Degree.
CLD	Chemiluminescence Detector
CO	Carbon Monoxide.
CO₂	Carbon Dioxide.
COV_IMEP	Coefficient of Variation of IMEP.
(CO₂%)_{intake}	CO ₂ concentration in the intake manifold.
(CO₂%)_{exhaust}	CO ₂ concentration in the exhaust manifold.
DAQ	Data Acquisition
DOC	Diesel Oxidation Catalyst.
ECR	Effective Compression Ratio.
ECU	Electronic Control Unit.
EGR	Exhaust Gas Recirculation.
eEGR	External Exhaust Gas Recirculation.
EGT	Exhaust Gas Temperature.
EVO	Exhaust Valve Opening.
FID	Flame Ionization Detector
FSN	Filter Smoke Number.
FS	Full Scale
GHG	Greenhouse Gas.
HRR	Heat Release Rate.
HC	Hydrocarbons.
HD	Heavy Duty.
iEGR	Internal Exhaust Gas Recirculation.
IMEP	Indicated Mean Effective Pressure.
IVO	Intake Valve Opening.
IVC	Intake Valve Closing
ISsoot	Net Indicated Specific Emissions of Soot.
ISNOx	Net Indicated Specific Emissions of NOx.
ISCO	Net Indicated Specific Emissions of CO.
ISHC	Net Indicated Specific Emissions of Unburned HC.
LIVC	Late Intake Valve Closing.
MFB	Mass Fraction Burnt
NDIR	Non-Dispersive Infrared Absorption
NOx	Nitrogen Oxides.
NIE	Net Indicated Efficiency
SCR	Selective Catalytic Reduction.
SOI	Start of Injection.
SOC	Start of Combustion.
TDC	Firing Top Dead Centre.
VVA	Variable Valve Actuation.
WHSC	World Harmonized Stationary Cycle.

References

1. Heywood J.B, "Internal Combustion Engine Fundamentals," ISBN 007028637X, 1988.
2. Kimura, S., Kimura, S., Aoki, O., Aoki, O., Ogawa, H., Ogawa, H., Muranaka, S., Muranaka, S., Enomoto, Y., and Enomoto, Y., "New combustion concept for ultra-clean and high-efficiency small DI diesel engines," *SAE Pap. 1999-01-3681* 3pp(724):01-3681, 1999, doi:10.4271/1999-01-3681.
3. Environmental Protection Agency and National Highway Traffic Safety

- Administration, "Greenhouse Gas Emissions and Fuel Efficiency Standards for Medium and Heavy-Duty Engines and Vehicles - Phase 2," *Fed. Regist.* 81(206):73478-74274, 2016, doi:<http://www.nhtsa.gov/Laws+&+Regulations/CAFE+-+Fuel+Economy/Fuel+economy+and+environment+label>.
4. Johnson, T. and Joshi, A., "Review of Vehicle Engine Efficiency and Emissions," *SAE Tech. Pap. Ser. 1*, 2018, doi:10.4271/2018-01-0329.
 5. California Air Resources Board, "Heavy-Duty Low-NOx and Phase 2 GHG Plans," <https://www.arb.ca.gov/msprog/hdlownox/hdlownox.htm>.
 6. Buckendale, L.R., Stanton, D.W., and Stanton, D.W., "Systematic Development of Highly Efficient and Clean Engines to Meet Future Commercial Vehicle Greenhouse Gas Regulations," *SAE Int.* 2013-01-2421, 2013, doi:10.4271/2013-01-2421.
 7. Stadlbauer, S., Waschl, H., Schilling, A., and Re, L. del, "Temperature Control for Low Temperature Operating Ranges with Post and Main Injection Actuation," 2013, doi:10.4271/2013-01-1580.
 8. Gehrke, S., Kovács, D., Eilts, P., Rempel, A., and Eckert, P., "Investigation of VVA-Based Exhaust Management Strategies by Means of a HD Single Cylinder Research Engine and Rapid Prototyping Systems," *SAE Tech. Pap.* 01(0587):47-61, 2013, doi:10.4271/2013-01-0587.
 9. Johnson, T., "Vehicular Emissions in Review," *SAE Int. J. Engines* 9(2):2016-01-0919, 2016, doi:10.4271/2016-01-0919.
 10. Miller, R., "Supercharged Engine," *United States Patents* (US 2 817 322), 1957.
 11. Parks, J., Huff, S., Kass, M., and Storey, J., "Characterization of in-cylinder techniques for thermal management of diesel aftertreatment," *SAE Pap.* (724):01-3997, 2007, doi:10.4271/2007-01-3997.
 12. Honardar, S., Busch, H., Schnorbus, T., Severin, C., Kolbeck, A., and Korfer, T., "Exhaust Temperature Management for Diesel Engines Assessment of Engine Concepts and Calibration Strategies with Regard to Fuel Penalty," *SAE Tech. Pap.*, 2011, doi:10.4271/2011-24-0176.
 13. Mayer, A., Lutz, T., Lämmle, C., Wyser, M., and Legerer, F., "Engine Intake Throttling for Active Regeneration of Diesel particle," *SAE Tech. Pap.* (724), 2003, doi:10.4271/2003-01-0381.
 14. Imperato, M., Antila, E., Sarjovaara, T., Kaario, O., Larmi, M., Kallio, I., and Isaksson, S., "NOx Reduction in a Medium-Speed Single-Cylinder Diesel Engine using Miller Cycle with Very Advanced Valve Timing," *SAE Tech. Pap.* 4970, 2009, doi:10.4271/2009-24-0112.
 15. Benajes, J., Molina, S., Martín, J., and Novella, R., "Effect of advancing the closing angle of the intake valves on diffusion-controlled combustion in a HD diesel engine," *Appl. Therm. Eng.* 29(10):1947-1954, 2009, doi:10.1016/j.applthermaleng.2008.09.014.
 16. Guan, W., Pedrozo, V., Zhao, H., Ban, Z., and Lin, T., "Investigation of EGR and Miller Cycle for NOx Emissions and Exhaust Temperature Control of a Heavy-Duty Diesel Engine," *SAE Tech. Pap.*, 2017, doi:10.4271/2017-01-2227.

17. Ding, C., Roberts, L., Fain, D.J., Ramesh, A.K., Shaver, G.M., McCarthy, J., Ruth, M., Koeberlein, E., Holloway, E.A., and Nielsen, D., "Fuel efficient exhaust thermal management for compression ignition engines during idle via cylinder deactivation and flexible valve actuation," *Int. J. Engine Res.* 17(6):619–630, 2016, doi:10.1177/1468087415597413.
18. Kim, J. and Bae, C., "An investigation on the effects of late intake valve closing and exhaust gas recirculation in a single-cylinder research diesel engine in the low-load condition," *Proc. Inst. Mech. Eng. Part D J. Automob. Eng.* 230(6):771–787, 2016, doi:10.1177/0954407015595149.
19. Pedrozo, V.B., May, I., Lanzanova, T.D.M., and Zhao, H., "Potential of internal EGR and throttled operation for low load extension of ethanol–diesel dual-fuel reactivity controlled compression ignition combustion on a heavy-duty engine," *Fuel* 179:391–405, 2016, doi:10.1016/j.fuel.2016.03.090.
20. Fessler, H. and Genova, M., "An Electro-Hydraulic 'Lost Motion' VVA System for a 3.0 Liter Diesel Engine," 2004(724), 2004, doi:10.4271/2004-01-3018.
21. Korfer, T., Busch, H., Kolbeck, A., Severin, C., Schnorbus, T., and Honardar, S., "Advanced Thermal Management for Modern Diesel Engines - Optimized Synergy between Engine Hardware and Software Intelligence," *Proc. Asme Intern. Combust. Engine Div. Spring Tech. Conf. 2012* 415–430, 2012, doi:10.1115/ICES2012-81003.
22. Guan, W., Zhao, H., Ban, Z., and Lin, T., "Exploring alternative combustion control strategies for low-load exhaust gas temperature management of a heavy-duty diesel engine," *Int. J. Engine Res.* 146808741875558, 2018, doi:10.1177/1468087418755586.
23. Ladommatos, N., Abdelhalim, S.M., Zhao, H., and Hu, Z., "The Dilution , Chemical , and Thermal Effects of Exhaust Gas Recirculation on Diesel Engine Emissions - Part 4: Effects of Carbon Dioxide and Water Vapour," (412), 1997.
24. Asad, U. and Zheng, M., "Exhaust gas recirculation for advanced diesel combustion cycles," *Appl. Energy* 123:242–252, 2014, doi:10.1016/j.apenergy.2014.02.073.
25. Zhao, C., Yu, G., Yang, J., Bai, M., and Shang, F., "Achievement of Diesel Low Temperature Combustion through Higher Boost and EGR Control Coupled with Miller Cycle," (x), 2015, doi:10.4271/2015-01-0383.
26. Sjöblom, J., "Combined Effects of Late IVC and EGR on Low-load Diesel Combustion," *SAE Int. J. Engines* 8(1):2014-01-2878, 2014, doi:10.4271/2014-01-2878.
27. Verschaeren, R., Schaepdryver, W., Serruys, T., Bastiaen, M., Vervaeke, L., and Verhelst, S., "Experimental study of NOx reduction on a medium speed heavy duty diesel engine by the application of EGR (exhaust gas recirculation) and Miller timing," *Energy* 76(x):614–621, 2014, doi:10.1016/j.energy.2014.08.059.
28. Stricker, K., Kocher, L., Koeberlein, E., Alstine, D. Van, and Shaver, G.M., "Estimation of effective compression ratio for engines utilizing flexible intake valve actuation," *Proc. Inst. Mech. Eng. Part D J. Automob. Eng.* 226(8):1001–1015, 2012, doi:10.1177/0954407012438024.

29. AVL., "AVL 415SE Smoke Meter," *Prod. Guid. Graz, Austria*; 1-4, 2013.
30. Regulation No 49 – uniform provisions concerning the measures to be taken against the emission of gaseous and particulate pollutants from compression-ignition engines and positive ignition engines for use in vehicles. Off J Eur Union, 2013.
31. Zhao, H., "HCCI and CAI engines for the automotive industry," ISBN 9781855737426, 2007.
32. Charlton, S., Dollmeyer, T., and Grana, T., "Meeting the US Heavy-Duty EPA 2010 Standards and Providing Increased Value for the Customer," *SAE Int. J. Commer. Veh.* 3(1):101-110, 2010, doi:10.4271/2010-01-1934.
33. Johnson, T. V., "Diesel Emissions in Review," *SAE Int. J. Engines* 4(1):143-157, 2011, doi:10.4271/2011-01-0304.
34. Chatterjee, S., Naseri, M., and Li, J., "Heavy Duty Diesel Engine Emission Control to Meet BS VI Regulations," *SAE Tech. Pap.* (x), 2017, doi:10.4271/2017-26-0125.

Appendix A. Test cell measurement devices

Variable	Device	Manufacturer	Measurement range	Linearity/Accuracy
Speed	AG 150 Dynamometer	Froude Hofmann	0-8000 rpm	± 1 rpm
Torque	AG 150 Dynamometer	Froude Hofmann	0-500 Nm	± 0.25% of full scale (FS)
Diesel flow rate (supply)	Proline promass 83A DN01	Endress+Hauser	0-20 kg/h	± 0.10% of reading
Diesel flow rate (return)	Proline promass 83A DN02	Endress+Hauser	0-100 kg/h	± 0.10% of reading
Intake air mass flow rate	Proline t-mass 65F	Endress+Hauser	0-910 kg/h	± 1.5% of reading
In-cylinder pressure	Piezoelectric pressure sensor Type 6125C	Kistler	0-300 bar	≤ ± 0.4% of FS
Intake and exhaust pressures	Piezoresistive pressure sensor Type 4049A	Kistler	0-10 bar	≤ ± 0.5% of FS
Oil pressure	Pressure transducer UNIK 5000	GE	0-10 bar	< ± 0.2% FS
Temperature	Thermocouple K Type	RS	233-1473K	≤ ± 2.5 K

Intake valve lift	S-DVRT-24 Displacement Sensor	LORD MicroStrain	0-24 mm	$\pm 1.0\%$ of reading using straight line
Smoke number	415SE	AVL	0-10 FSN	-
Fuel injector current signal	Current Probe PR30	LEM	0-20A	± 2 mA